Eur. J. Mech. B/Fluids 18 (1999) 931–957

Over-reflection and instabilities in shear flows of shallow water with bottom friction

P.A. Yakubenko, G.A. Shugai

Department of Hydraulic Engineering, The Royal Institute of Technology, 10044 Stockholm, Sweden

(Received 13 March 1998; revised and accepted 25 January 1999)

Abstract – In a two-dimensional shear flow of shallow water, the bottom friction relates uniquely the spanwise profile of the depth-averaged velocity to the bottom topography. If the basic flow varies weakly in the spanwise direction, the local analysis of stability at every spanwise position gives the region of the flow parameters for which the classic hydraulic instability due to the bottom friction cannot occur. In this region, the linear analyses of the waves scattering and instability due to the lateral shear can be performed effectively by means of the frictionless linearized equations if both the bottom slope and friction are equally small.

The energy of the total perturbed flow can be split into three main parts that correspond to the basic flow, small amplitude wave motion and induced mean flow. The waves can be either amplified or damped near the critical layers, where their streamwise phase velocity equals the velocity of the basic flow. Two physical mechanisms of this amplification exist. The first one is similar to that suggested by Takehiro and Hayashi for a linear frictionless shallow water flow. The incident and transmitted waves carry energy of opposite signs, which results in an increase in the amplitude of the reflected wave compared to that of the incident one. This mechanism of over-reflection operates for any combination of the flow parameters. The other mechanism is similar to Landau damping in plasma flows; it is related to the energy exchange between the waves and fluid particles at the critical layers due to the velocity synchronism. It may lead to either additional amplification or damping of the waves for different flow conditions. In particular, its significance can be reduced by stronger bottom friction. If the basic flow has uniform potential vorticity, Landau damping is negligible, and over-reflection always occurs. If the feed-back is provided by another critical layer, the net over-reflection results in the formation of trapped modes. © 1999 Éditions scientifiques et médicales Elsevier SAS

over-reflection / shallow water / shear flow / bottom friction

1. Introduction

The shallow-water approximation is based on the assumption that the horizontal lengthscale of the flow (e.g. the typical wavelength) is much larger than the typical depth. It provides a useful, if not crucial, reduction of dimensions in many hydraulic and geophysical applications. Thus, the vertical direction is eliminated from consideration by averaging the equations of motion over the flow depth. The shear stresses in the horizontal plane result then in friction at the bottom. The instability that is caused by the friction is often referred to as hydraulic; its most recognized consequence is the formation of roll waves in steep open channels and other hydraulic structures (Jeffreys [1]). It can occur even if the flow is uniform, i.e. if the bottom is an inclined plane.

If the depth-averaged basic flow varies in the spanwise direction, the other type of instability can occur (Satomura [2], Chu et al. [3], Takehiro and Hayashi [4], Dodd [5], Knessl and Keller [6]). The instability mechanism is based on the wave amplification near the critical layers, where the streamwise phase speed of the waves equals to the local streamwise velocity of the basic flow. In a wave scattering problem, the amplification appears in the form of over-reflection—the amplitude of the wave reflected from the critical layer is higher than that of the incident one. Strictly speaking, the viscous analysis is required near the critical layer. However, the instability can be efficiently predicted by pure inviscid theory if one treats properly the singularity that may occur in the inviscid equations.

For a linear shear flow of shallow water along a frictionless horizontal plane, Knessl and Keller [6] (hereafter referred to as KK) have obtained an exact analytic solution for small disturbances. In Section 7 of the present paper, we show how this solution can be adapted for a more realistic flow of shallow water, for which the bottom slope and friction are not negligible. KK have computed explicitly the reflection and transmission coefficients that satisfy a remarkably simple relation $|R|^2 = 1 + |T|^2$, which indicates over-reflection for any combination of the flow parameters.

If the bottom is a surface whose elements are inclined at the same angle to the horizon, the undisturbed profile of the depth-averaged velocity is uniquely related to the spanwise variation of the bottom. Furthermore, this relation can be taken as the only effect on the motion of small amplitude waves if both the bottom friction and slope are equally small. Using this approach, we generalize in the present paper the analysis of KK into the case of an arbitrary, weak variation of the bottom. However, we do not perform the straightforward matching procedure that has been proposed by them and was used earlier in their study of a rotating shear flow (Knessl and Keller [7]). Instead, we utilize the combination of the comparison equation technique with the matching of the WKBJ approximation in the complex plane, which was developed by Gavrilenko and Zelekson [8] and Basovich and Tsimring [9] (hereafter referred to as BT).

In recent years, the problem of stability of spatially developing flows has attracted much attention in fluid dynamics (e.g. Le Dizès et al. [10], Yakubenko [11], Brevdo and Bridges [12], among several others; an account of earlier results can be found in the review by Huerre and Monkewitz [13]). One of the central questions in these studies was how the local properties of the flow are related to its global stability. In particular, Brevdo and Bridges [12] have shown by means of mathematical examples that the presence of a region of local instability is not necessary for the global instability. In Section 8 of the present paper, we support their conclusion by demonstrating that over-reflection provides an instability mechanism that requires no local amplification except at the critical layers.

2. Formulation

The basic flow is a free surface stream of an incompressible fluid. The bottom is a cylindric surface with the elements inclined at angle θ to the horizon. The frame of reference is Cartesian and related to the undisturbed free surface that is plane (*figure 1*). The flow depth can be measured normally to the free surface if the bottom slope is small. Thus, the depth of the basic flow is $H(y)$ that is made dimensionless by the typical depth H_{typ}. Whether the flow is turbulent or of a laminar nature is not specified. However, the vertical variation of the flow parameters is assumed to be negligible, and it does not affect the depth-averaged equations, which is more representative of turbulent flows. The depth-averaged velocity of the basic flow has only one (streamwise) non-zero component $U(y) > 0$ that is made dimensionless by the typical velocity U_{typ}.

For the disturbances, the typical wavelength $l_{\text{typ}} \gg H_{\text{typ}}$, and the typical phase speed is of the order U_{typ}. The effects of the surface tension and the medium above the free surface are assumed to be negligible. The Saint Venant shallow-water equations that are made dimensionless by means of the fluid density ρ, H_{typ} and U_{typ} can be written in the following form:

$$\partial_t(h_* - H) + \nabla \cdot (h_* \mathbf{u}_*) = 0, \tag{1}$$

$$\partial_t \mathbf{u}_* + (\mathbf{u}_* \cdot \nabla)\mathbf{u}_* = -F^{-2}\nabla(h_* - H) + F^{-2}\tan(\theta)\mathbf{e}_x - \tau h_*^{-1}, \tag{2}$$

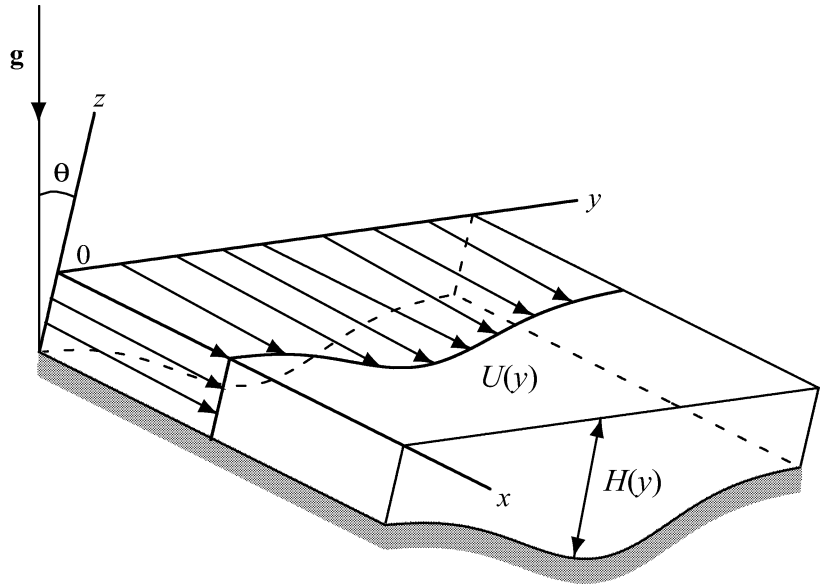

Figure 1. Flow geometry.

in which h_* is the flow depth, $\mathbf{u}_*$ is the depth-averaged velocity vector, $\nabla \equiv [\partial_x, \partial_y]$, and the Froude number is introduced from

$$F^2 = \frac{U_{\mathrm{typ}}^2}{H_{\mathrm{typ}} g \cos(\theta)}.$$

The bottom friction is given by

$$\tau = \lambda \mathbf{u}_* f\left(|\mathbf{u}_*|\right), \tag{3}$$

in which λ is a non-dimensional friction factor, and $f(|\mathbf{u}_*|)$ is an arbitrary function such that $f > 0$ and $f' > 0$. Equation (3) generalizes some of ad hoc formulas that are used in applications (Chu et al. [3], Grubišić and Smith [14], Chen and Jirka [15], Yakubenko and Shugai [16], among recent ones).

The total flow is presented as

$$h_* = H(y) + h(x, y, t)a + h^{(2)}(x, y, t)a^2,$$
$$\mathbf{u}_* = \left[U(y), 0\right] + \left[u(x, y, t), v(x, y, t)\right]a + \left[u^{(2)}(x, y, t), v^{(2)}(x, y, t)\right]a^2,$$

in which $a \ll 1$ stands for the typical amplitude. The quantities h, u and v are associated with the motion of small amplitude waves—they are what actually appear in the linearized equations of motion—the terms $h^{(2)}$, $u^{(2)}$ and $v^{(2)}$ are lumped into the so-called induced mean motion; in contrast to those for waves, they may have non-zero mean values with respect to the waves period.

If $\lambda = \mathrm{O}(1)$, Eqs (1) and (2) give

$$a^0: \quad F^{-2}\tan(\theta) - \Upsilon = 0, \tag{4}$$

$$a^1: \quad Dh + (\partial_x u + \partial_y v)H + H'v = 0, \tag{5}$$

$$Du + U'v = -F^{-2}\partial_x h - \Upsilon_h h - \Upsilon_u u, \tag{6}$$

$$Dv = -F^{-2}\partial_y h - \Upsilon_v v, \tag{7}$$

in which $D \equiv \partial_t + U\partial_x$,

$$\Upsilon = H^{-1}\lambda U f(U), \qquad \Upsilon_h = -H^{-2}\lambda U f(U),$$

$$\Upsilon_u = H^{-1}\lambda\left[f(U) + Uf'(U)\right], \qquad \Upsilon_v = H^{-1}\lambda f(U),$$

and primes stand for derivatives of single-argument functions.

If normal mode decomposition is performed as

$$[h, u, v] = \left[\hat{h}(y), \hat{u}(y), \hat{v}(y)\right] \exp(ik_x x - i\omega t),$$

Eqs (5)–(7) yield

$$\hat{u} = \frac{k_x F^{-2} - i\Upsilon_h}{\Omega + i\Upsilon_u}\hat{h} - \frac{U' F^{-2}}{(\Omega + i\Upsilon_u)(\Omega + i\Upsilon_v)}\hat{h}', \qquad \hat{v} = -i\frac{F^{-2}}{\Omega + i\Upsilon_v}\hat{h}', \tag{8}$$

$$\hat{h}'' - \left\{\partial_y\left[\log\left(\Lambda^2\right)\right] - \frac{i\partial_y\Upsilon_u}{\Omega + i\Upsilon_u}\right\}\hat{h}' + k_y^2\hat{h} = 0, \tag{9}$$

in which

$$\Lambda^2 = (\Omega + i\Upsilon_u)(\Omega + i\Upsilon_v)k_x^{-2}H^{-1},$$

$$k_y^2(y) = k_x^2\left[F^2\Lambda^2 - 1 + iF^2\left(k_x^{-1}\Upsilon_h - \frac{\Upsilon_v\Lambda^2}{\Omega + i\Upsilon_v}\right)\right]\frac{\Omega + i\Upsilon_v}{\Omega + i\Upsilon_u}, \tag{10}$$

and $\Omega(y) = \omega - k_x U(y)$.

3. Uniform flow: the limits of the approach

If the flow is uniform ($U = H = 1$), Eqs (4) and (9) yield

$$\lambda F^2 f(1) = \tan(\theta), \tag{11}$$

$$\hat{h}'' + k_y^2\hat{h} = 0.$$

Equation (10) gives the dispersion relation if k_y is treated as the wavenumber in the y-direction. The dispersion relation is polynomial of the third order in ω. For $|k_x| \gg 1$, its temporal branches that can be presented as

$$\omega_0 = k_x - i\Upsilon_v + \mathrm{O}\left(k_x^{-1}\right),$$

$$\omega_m = \left[1 + (-1)^m F^{-1}\right]k_x - \frac{1}{2}i\left[\Upsilon_u + (-1)^m\Upsilon_h F\right] + \mathrm{O}\left(k_x^{-1}\right), \tag{12}$$

in which $m = 1$ or 2. (Note that the leading order terms are independent of k_y.) Since $\Upsilon_u > 0$ and $\Upsilon_h < 0$, Eq. (12) indicates that the flow is unstable for $F > -\Upsilon_u\Upsilon_h^{-1}$, which can be rewritten by using (11) in the following equivalent form:

$$\tan(\theta) > \lambda\left[f(1) + f'(1)\right]^2 f^{-1}(1). \tag{13}$$

Furthermore, in the case of instability, (12) reveals that disturbances of infinitely short wavelength are amplified. One may argue that this fact contradicts the long-wave nature of the shallow water approximation. The problem is resolved if the internal lateral friction is taken into account in addition to the bottom friction (e.g. Grubišić and Smith [14]). However, this requires other terms of higher order in $H_{\text{typ}} l_{\text{typ}}^{-1}$ to be retained (Yakubenko and Shugai [16]). Since our primary goal is to analyze how the bottom friction influences the shear instability, we do not attempt further complication of the equations. Instead, in the following treatment, we assume that (13) is not satisfied.

4. Frictionless horizontal bottom

The other important limiting case is a flow along a horizontal frictionless plane, i.e. the case $\theta = \lambda = 0$. Equation (9) then gives

$$\hat{h}'' - \partial_y \left[\log(\Lambda^2)\right]\hat{h}' + k_x^2 (F^2 \Lambda^2 - 1)\hat{h} = 0, \tag{14}$$

in which $c = \omega / k_x$ is the streamwise phase velocity, and $\Lambda^2 = (U - c)^2 H^{-1}$. Equation (14) is similar to those for shear flows of stratified fluids (Booker and Bretherton [17], BT [9]; see also Lindzen [18] and Lott et al. [19], and references therein) and for compressible gases with temperature variation (e.g. Zhuang et al. [20]).

Since (4) disappears, the depth and velocity of the basic flow can vary independently. Thus, choosing $H(y)$ and/or $U(y)$, one can get virtually any result. Several particular cases have been discussed by Mei [21]. In Appendix A, we suggest a relatively systematic way to look for analytically solvable cases.

If the bottom is uniform ($H = 1$), Eq. (14) yields

$$\hat{h}'' - 2U'(U - c)^{-1}\hat{h}' + k_x^2 \left[F^2 (U - c)^2 - 1\right]\hat{h} = 0. \tag{15}$$

In shallow water, this equation was investigated first by Satomura [2]. However, mathematically similar equations had been studied earlier in gas dynamics and acoustics (see Gavrilenko and Zelekson [5], Drazin and Davey [22], and references therein).

For the case $U(y) \equiv y$, Takehiro and Hayashi [4] investigated numerically how a wave packet interacts with the critical layer. More recently, Knessl and Keller [6] have obtained an exact solution of the wave scattering problem. These studies have shown that over-reflection occurs for any combination of the parameters.

It must be noted that even in the frictionless case, the velocity profile can be related uniquely to the bottom topography if the entire flow is subjected to rotation. The effect may be significant in many geophysical applications (Hayashi and Young [23], Knessl and Keller [7]; see also McPhaden and Ripa [24] for a review).

5. Weak friction

We assume that both the bottom friction and slope are equally small in the following sense:

$$\gamma^2 = \lambda \cot(\theta) = \mathrm{O}(1), \quad \lambda = \mathrm{O}\left(a^{1+\nu}\right), \tag{16}$$

in which $0 < \nu < 1$. The latter inequality insures that the friction does not affect the equations for perturbations up to $\mathrm{O}(a^2)$. However, if one intends to use also higher order approximations, more precise choice of ν may be required.

Equations (1) and (2) together with (16) yield

$$a^1: \quad Dh + H(\partial_x u + \partial_y v) + H'v = 0, \tag{17}$$

$$Du + U'v = -F^{-2}\partial_x h, \tag{18}$$

$$Dv = -F^{-2}\partial_y h, \tag{19}$$

$$a^{1+\nu}: \quad H = \gamma^2 F^2 U f(U). \tag{20}$$

The equations for the induced mean flow are not presented here, since we intend to use the flow only as an ‘energy reservoir’ without looking at its particular details.

Equations (17)–(20) give

$$\hat{h}'' - \partial_y\left[\log(\Lambda^2)\right]\hat{h}' + k_x^2\left(\gamma^{-2}\Lambda^2 - 1\right)\hat{h} = 0, \tag{21}$$

in which

$$\Lambda^2(y) = \frac{[U(y) - c]^2}{U(y) f[U(y)]}. \tag{22}$$

Thus, in the leading order approximation, the problem is similar to that of the frictionless case. However, the depth and velocity of the basic flow cannot vary independently any more. Most of the following treatment is based on Eq. (21). However, we pose few restrictions as a legacy of the original problem.

First, we assume that hydraulic instability does not occur. According to (13) and (14), this is possible only if

$$\gamma^2 > F^{-1}\left[f(U) + U f'(U)\right]^{-1}. \tag{23}$$

Second, if the terms due to the bottom friction are dropped in (5)–(7), the resulting reduced equations possesses the following particular solution:

$$v = v_0, \qquad h(t) = h_0 - H'v_0 t, \qquad u(t) = u_0 - U'v_0 t, \tag{24}$$

in which $h_0,\ u_0$ and v_0 are arbitrary constants. Solutions of this kind are often referred to as the algebraic instability that is caused by the lift-up effect (for more details see e.g. Henningson et al. [25]). They are removed if the friction terms are retained. Therefore, dealing with the reduced equations, we prohibit them formally. However, it may be noted that the lift-up effect is a physical mechanism that may operate as well in the general case.

The final restriction concerns the critical layers $y = y_c$, where the velocity of the basic flow equals the phase speed of the waves, i.e. $U(y_c) = c$. Because of its particular importance, we will discuss it more thoroughly in the following section.

5.1. Bypass rule

Equation (21) has a singularity at $y = y_c$. As a result, its solution has there a branch point. (A more general treatment of the problem and an overview of related works were presented by Grimshaw [26].) Therefore, the problem of choice of the proper branch may arise. However, the choice can be made easily if one keeps in mind that (21) can be obtained from (9) by neglecting the friction terms; the latter equation shows that the actual position of the singularity is given by

$$y = y_c + i\frac{\Upsilon_u(y_c)}{k_x U'(y_c)} + \mathrm{O}\left(\lambda^2\right), \tag{25}$$

where $\Upsilon_u = \mathrm{O}(\lambda)$. Hence, the solutions of the reduced Eq. (21) at the real y-axis can be matched around y_c in the complex y-plane. Furthermore, since $\Upsilon_u > 0$, Eq. (25) shows that the bypass must be taken in the lower complex half-plane for $k_x U'(y_c) > 0$, and in the upper one for $k_x U'(y_c) < 0$.

An alternative approach is based on the rule that was introduced by Landau [27] in plasma physics and by Lin [28] in fluid dynamics (the references can be found in Boyd [29], Stepanyants and Fabrikant [30], Le Dizès et al. [31]). Hence, for $\mathrm{Im}(\omega) = 0$, the singularity at the real axis can be bypassed in the complex plane in the same manner as it is bypassed by the real axis for $\mathrm{Im}(\omega) > 0$. Note that the application of the rule depends on the form in which the normal mode decomposition is taken. In particular, it must be reversed if the factor $\exp(i\omega t)$ is used instead of $\exp(-i\omega t)$.

5.2. Energetics

Since the energy and momentum of disturbances are quantities that are quadratic in the amplitude, their definitions in the framework of the linear analysis may be not intuitive. One of the least ambiguous ways is the following (e.g. Hayashi and Young [23], McPhaden and Ripa [24]). The total densities of the energy and x-component of momentum are introduced as

$$E_* = \frac{1}{2}\overline{h_*\left(u_*^2 + v_*^2\right) + F^{-2}(h_* - H)^2} \quad \text{and} \quad M_* = \overline{h_* u_*},$$

respectively, in which the bars denote the average in the x-direction (over the wave period). They can be presented in the following form:

$$E_* = \frac{1}{2}HU^2 + \left(E + E^{(2)}\right)a^2 + \mathrm{O}\left(a^4\right),$$
$$M_* = UH + \left(M + M^{(2)}\right)a^2 + \mathrm{O}\left(a^4\right),$$

in which $M = \overline{hu}$, and

$$E = \mathcal{E} + UM \tag{26}$$

with

$$\mathcal{E} = \frac{1}{2}H\left(\overline{u^2} + \overline{v^2}\right) + \frac{1}{2}F^{-2}\overline{h^2}.$$

(Thus introduced, E and M are often called pseudoenergy and pseudomomentum, and only the part $\mathcal{E}$ is taken as the wave energy.) The energy and momentum of the induced mean flow are given by

$$E^{(2)} = \frac{1}{2}U^2\overline{h^{(2)}} + HU\overline{u^{(2)}}, \qquad M^{(2)} = H\overline{u^{(2)}} + U\overline{h^{(2)}}.$$

Equations for E and M can be obtained by manipulating the linearized Eqs (17)–(19). Hayashi and Young [23] and McPhaden and Ripa [24] have described the required procedure in great detail, including some hints due to the original non-linear problem. Here, we discuss only the final results that are important in our treatment. Thus,

$$\partial_t M + H^2\overline{vq} = \partial_y(-H\overline{uv}), \tag{27}$$
$$\partial_t E + UH^2\overline{vq} = c\partial_y(-H\overline{uv}). \tag{28}$$

Therefore, the energy and momentum fluxes can be related to the Reynolds stress $-H\overline{uv}$ induced by the wave motion. There are two important particular cases, for which Equations (27) and (28) can be further transformed into the form of conservation laws.

Equations (17)–(19) yield

$$Dq = -Q'v, \tag{29}$$

in which the potential vorticity of the basic flow and waves are given by $Q = -U'H^{-1}$ and $q = (\partial_x v - \partial_y u - Qh)H^{-1}$, respectively. If the potential vorticity of the waves is initially zero, (29) can be integrated to give $q = -Q'\eta$, in which the lateral displacement of the fluid particles is introduced from $D\eta = v$. Equations (27) and (28) give

$$\partial_t M_d = \partial_y(-H\overline{uv}), \tag{30}$$

$$\partial_t E_d = c\partial_y(-H\overline{uv}), \tag{31}$$

in which

$$M_d = M - \frac{1}{2}H^2 Q'\overline{\eta^2}, \qquad E_d = E - \frac{1}{2}UH^2 Q'\overline{\eta^2}. \tag{32}$$

Hayashi and Young [23] have related the terms proportional to $\overline{\eta^2}$ to the induced mean motion. However, an actual relation between them and $E^{(2)}$ and $M^{(2)}$ is hardly expected in the general case (for further discussion see Craik [32, Section 11.4]).

Equations (30) and (31) yield

$$E_d - cM_d = G(y),$$

in which $G(y)$ is an arbitrary function. If $G(y) \equiv 0$ is provided by the initial conditions, one has $E_d = cM_d$. Furthermore, if the potential vorticity of the basic flow is uniform ($Q' = 0$), then $E_d = E,\ M_d = M$, and

$$\mathcal{E} = \frac{\omega - Uk_x}{\omega} E.$$

(The latter is a well known formula that relates energy and pseudoenergy, e.g. Acheson [33].) Since $\mathcal{E} > 0$, the density the wave energy E has different signs at the opposite sides of the critical layer. The same conclusion can be reached in the general case, and more rigorously, from the Lagrangian description of the wave motion (BT [9], Craik [32]; see also Ostrovskii et al. [34] for a review).

If $Q' \neq 0$, the equations for energy and momentum can be obtained from (27)–(29) in the form similar to (30) and (31) with

$$E_d = E - \frac{1}{2}UH^2(Q')^{-1}\overline{q^2}, \qquad M_d = M - \frac{1}{2}H^2(Q')^{-1}\overline{q^2}.$$

6. Scattering problem

For the sake of simplicity, we restrict attention to the following particular case:

$$f(U) \equiv U; \tag{33}$$

the corresponding law of the bottom friction is called the Chèzy formula, it has been used in hydraulic practice for more than a century. The instability condition (13) takes the celebrated form $\tan(\theta) > 4\lambda$ (Jeffreys [1]).

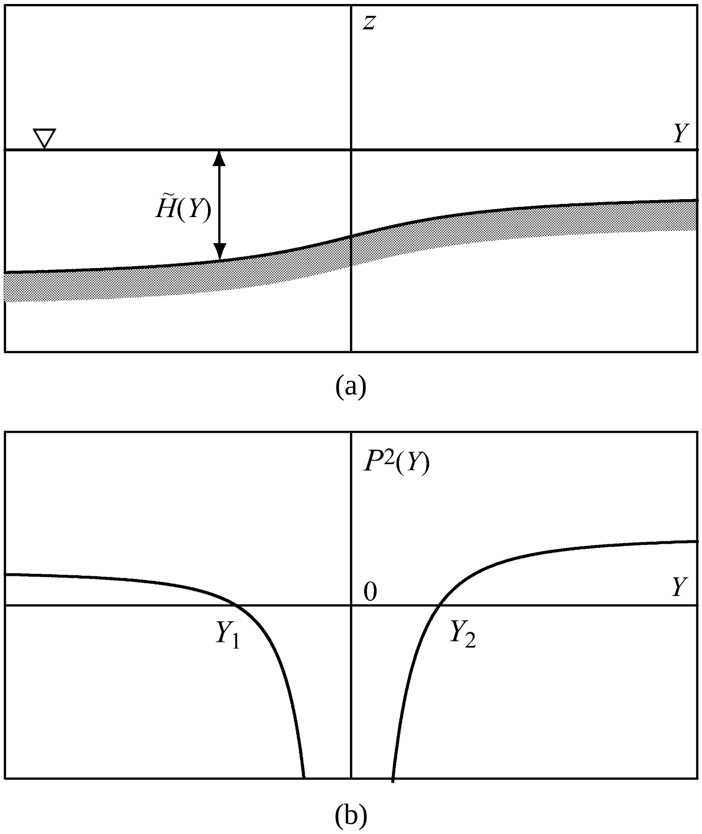

Figure 2. (a) Bottom profile and (b) the corresponding potential in the wave scattering problem.

Thus, for weak friction, the hydraulic instability is absent if

$$\gamma > 1/2. \tag{34}$$

The basic flow velocity is given by a monotonous function $U(y)$ such that $U(y \to \pm\infty) \to U_\pm = \text{const}$. The corresponding bottom topography is given by $H = \gamma^2 F^2 U^2$, *figure 2(a)*. The condition

$$(U_\pm - c)^2 > \gamma^2 U_\pm^2 \tag{35}$$

is necessary to allow the wave propagation at least for large $|y|$. If the incident wave may come from either direction ($y = \pm\infty$), the assumption

$$U'(y) > 0 \tag{36}$$

entails no loss of generality. We assume further that a critical layer occurs in the flow, which implies the inequality

$$0 < U_- < c < U_+. \tag{37}$$

Condition (35) leads then to

$$(1+\gamma)U_- < c < U_+(1-\gamma), \tag{38}$$

which in its turn implies the following restriction:

$$\gamma < \frac{U_+ - U_-}{U_+ + U_-} < 1. \tag{39}$$

Finally, (34) and (39) yield $U_+ > 3U_-$.

The local wavelength can be estimated as $l = \mathrm{O}(\gamma|k_x\Lambda|^{-1})$, and the local scale of the basic flow variation can be estimated as $L = \mathrm{O}[U(U')^{-1}]$. The shallow-water approximation requires $l_{\mathrm{typ}} \gg 1$. In addition to this, we assume that $l(y)L^{-1}(y) \ll 1$ everywhere, except maybe in a small neighborhood of the critical layer, which means that the basic flow varies weakly at the typical wavelength. This weak variation is made explicit by introducing $\widetilde{U}(Y) \equiv U(\varepsilon^{-1}Y + y_c)$ and $\widetilde{\Lambda}(Y) \equiv \Lambda(\varepsilon^{-1}Y + y_c)$, in which $\varepsilon = l_{\mathrm{typ}}L_{\mathrm{typ}}^{-1} \ll 1$, and the shifted slow coordinate is introduced as $Y = \varepsilon(y - y_c)$. The critical layer is then located at $Y = 0$. If a new unknown function is introduced as $\tilde{h}(Y) \equiv \hat{h}(\varepsilon^{-1}Y + y_c)\widetilde{\Lambda}^{-1}(Y)$, Eq. (21) takes the standard form

$$\tilde{h}'' + P^2(Y)\tilde{h} = 0, \tag{40}$$

in which the scattering potential is given by

$$P^2 = \varepsilon^{-2}k_Y^2 + \widetilde{\Lambda}^{-1}\widetilde{\Lambda}'' - 2\widetilde{\Lambda}^{-2}\big(\widetilde{\Lambda}'\big)^2 \tag{41}$$

that is sketched in *figure 2(b)*, $\widetilde{\Lambda}^2 = (1 - c\widetilde{U}^{-1})^2$, and $k_Y^2 = k_x^2(\gamma^{-2}\widetilde{\Lambda}^2 - 1)$.

The Laurent series expansion of (41) near $Y = 0$ gives

$$P^2(Y) = -2Y^{-2} - \widetilde{\Lambda}''(0)\big[\widetilde{\Lambda}'(0)\big]^{-1}Y^{-1} + \mathrm{O}(1), \tag{42}$$

which indicates that the origin is the second order pole. Furthermore, since $\Lambda(Y)$ tends to a constant as $Y \to \pm\infty$, one has

$$P^2 = \varepsilon^{-2}k_Y^2 + \mathrm{o}(1) \tag{43}$$

for $|Y| \gg 1$.

Zeros of function $k_Y^2(Y)$ are roots of the equation

$$k_x\widetilde{U}(Y) = \omega(1 \pm \gamma)^{-1}. \tag{44}$$

Because the velocity profile is monotonous and due to conditions (35) and (37), Eq. (44) has two real roots Y_m with $m = 1$ or 2. In addition, we assume that any possible complex zero of $k_Y^2(Y)$ is located far from the real Y axis. (Function $P^2(Y)$ may have complex zeros close to the origin, as (42) indicates.)

If the WKBJ approximation is used, $Y = Y_m$ are turning points. After Heading [35] and BT [9], we use the following notations:

$$(Y_m, Y) \equiv k_Y^{-1/2}(Y)\exp\left(i\varepsilon^{-1}\int_{Y_m}^{Y} k_Y(\xi)\,d\xi\right), \tag{45}$$

$$(Y, Y_m) \equiv k_Y^{-1/2}(Y)\exp\left(-i\varepsilon^{-1}\int_{Y_m}^{Y} k_Y(\xi)\,d\xi\right). \tag{46}$$

These expressions are often called elementary (or base) WKBJ solutions.

6.1. Direction of wave propagation

Application of formulas (45) and (46) requires again a choice of the branches, this time for $k_Y(Y)$. From the mathematical point of view, the choice may be arbitrary, as far as it is unique. However, a scattering problem requires precise identification of the incident and scattered waves. Since the exact solution must be treated for $\mathrm{Im}(\omega) = 0$ as a limiting case of that for $\mathrm{Im}(\omega) > 0$, it seems natural to take the branch cuts so that they do not cross the real Y axis for $\mathrm{Im}(\omega) > 0$, which separates the branches $\pm k_Y(Y)$ one from the other along the real axis. Equations (39) and (44) show that the turning points move for $\mathrm{Im}(\omega) > 0$ into the same complex half-plane as the pole does. Therefore, the branch cuts must be taken as shown in *figure 3*. Furthermore, the

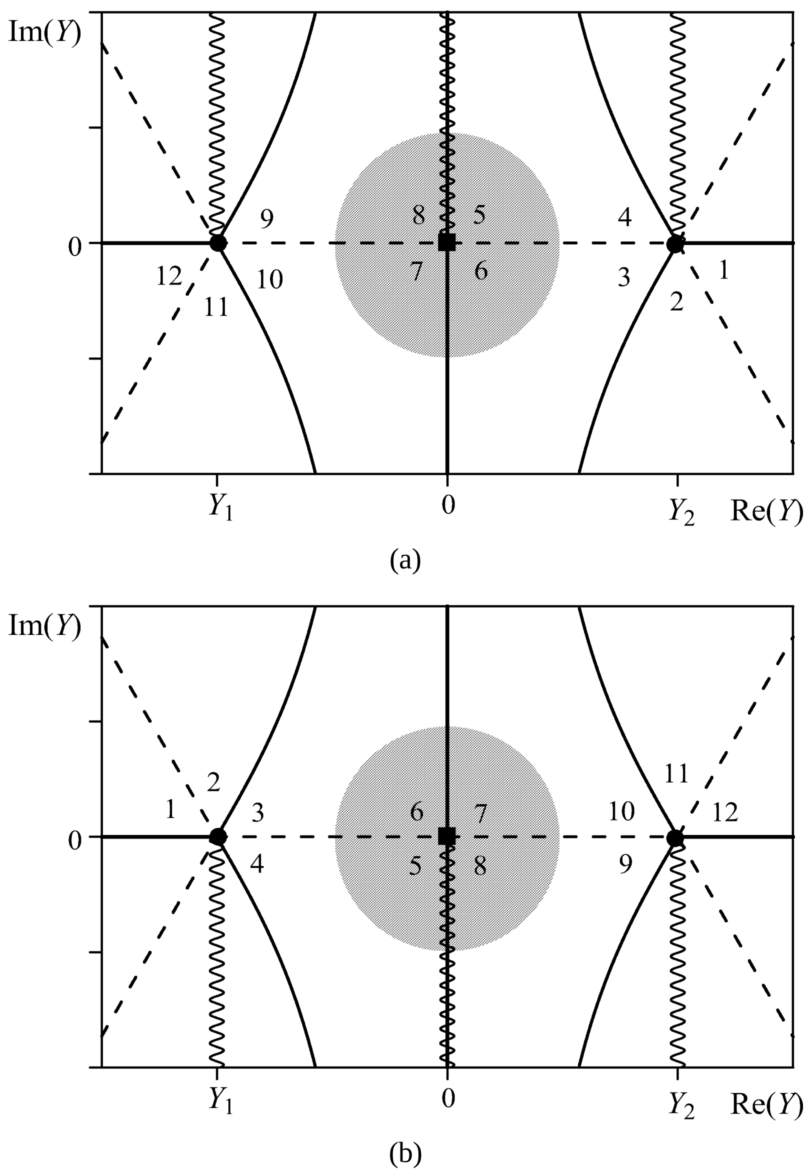

Figure 3. The Stokes and anti-Stokes lines are shown by the dashed and solid lines, respectively. The wavy lines are for the branch cuts. In the grey region, the solution is match by means of the comparison equation. Parts (a) and (b) correspond to $k_x > 0$ and $k_x < 0$, respectively.

elementary WKBJ solutions (Y_m, Y) and (Y, Y_m) can be easily identified as two waves that propagate in the opposite directions. For $\mathrm{Im}(\omega) = 0$, their directions of propagation are determined for the entire real Y axis by sign[Im(k_Y)] at the interval $Y_1 < Y < Y_2$. Actually, for $\mathrm{Im}(\omega) > 0$, both waves must be evanescent, which implies the same sign of $\mathrm{Im}[k_Y(Y)]$ for the entire real axis. For example, if $\mathrm{Im}(k_Y) < 0$ at $Y_1 < Y < Y_2$, the waves $\overleftarrow{(Y_m, Y)}$ and $\overrightarrow{(Y, Y_m)}$ propagate to the left and to the right, respectively. (Here and below, we use the arrows when it is important to indicate the direction of propagation.)

Another confirmation of the above choice is based on the following alternative approach (Booker and Bretherton [17]). Function $k_Y(Y)$ can be treated as the local wavenumber in the Y-direction. The directions of the wave propagation in the regions where $\mathrm{Im}[k_Y(Y)] = 0$ are related to the direction of the wave energy flux, and thus to the sign of the Y-component of the local group velocity

$$w_g(Y) \equiv \frac{\partial \omega}{\partial k_Y} = k_Y \Omega^{-1},$$

in which $\Omega(Y) = \omega - k_x \widetilde{U}(Y)$ presents the local frequency due to the Doppler shift. The wave (Y_m, Y) propagates to the right for $w_g > 0$, and to the left for $w_g < 0$. To demonstrate the connection between both approaches, let us consider the following case: $k_x < 0$ and $\arg(k_Y) = -\pi/2$ at $[Y_1, Y_2]$. Since $k_x \widetilde{U}'(0) < 0$ due to the assumption (36), the pole at $Y = 0$ must be bypassed in the upper complex half-plane. Matching around the turning points in the same half-plane (*figure 3(b)*) implies

$$\arg(k_Y) = \begin{cases} 0 & \text{for } Y < Y_1, \\ -\pi & \text{for } Y > Y_2. \end{cases}$$

Since $\mathrm{Im}(k_Y) < 0$ at $[Y_1, Y_2]$, the wave $\overleftarrow{(Y_m, Y)}$ propagates to the left according to the first approach. For $Y > Y_2$, one has $k_Y < 0$ and $\Omega(Y) > 0$, the latter condition is because the velocity profile is increasing and $\omega = k_x \widetilde{U}(0)$. Similarly, $k_Y > 0$ and $\Omega(Y) < 0$ for $Y < Y_1$. Hence, $w_g < 0$, which indicates the same (left) direction of propagation. It is worthwhile to observe that BT [9] did not follow the above described rule in their analysis. Thus, they matched the WKBJ approximation around turning points Y_1 and Y_2 in the opposite half-planes (BT [9, p. 245, figure 6]), which implies $\arg(k_Y) = 0$ for $Y < Y_1$ and $Y > Y_2$, and thus different signs of w_g in these regions.

6.2. Comparison equation

After Gavrilenko and Zelekson [8], we use the following equation:

$$\tilde{h}'' + \Pi^2(Y)\tilde{h} = 0, \tag{47}$$

in which

$$\Pi^2 = \varepsilon^{-2} k_Y^2 - (S')^2\left[2S^{-2} - \kappa S^{-1}\right] + \frac{1}{4} k_Y^{-2}\left[2k_Y k_Y'' - 3(k_Y')^2\right],$$

$$S(Y) \equiv 2i\varepsilon^{-1} \int_0^Y k_Y(\xi)\, d\xi. \tag{48}$$

If

$$\kappa = \frac{i\varepsilon \widetilde{\Lambda}''(0)}{2k_Y(0)\widetilde{\Lambda}'(0)}, \tag{49}$$

one has $\Pi^2 = P^2 + \mathrm{O}(1)$ for $|Y| \ll 1$. Therefore, Π^2 and P^2 have singularities of the same type at $Y = 0$. Moreover, $\Pi^2(Y) = \varepsilon^{-2} k_Y^2 + \mathrm{o}(1)$ for $|Y| \gg 1$, which is similar to (43). Hence, (47) presents a good approximation of the original equation (40); a more detailed mathematical treatment can be found in Olver [36, Section 11].

The solution of (47) can be presented as

$$\tilde{h}(Y) = k_Y^{-1/2}(Y)\zeta\left[S(Y)\right], \tag{50}$$

in which the new unknown function $\zeta(S)$ must satisfy the equation

$$\zeta'' + \left(-\frac{1}{4} + \kappa S^{-1} - 2S^{-2}\right)\zeta = 0, \tag{51}$$

which is Whittaker's equation. Its general solution can be expressed in terms of Whittaker's functions as

$$\zeta = C W_{\kappa,\mu}(S) + D W_{-\kappa,\mu}(-S), \tag{52}$$

in which C and D are arbitrary constants, and $\mu = 3/2$.

6.3. *Stokes phenomenon*

The solution (40) breaks down near the points Y_1 and Y_2. However, since those are simple turning points, the standard WKBJ matching technique can be used. We will refer to the curves defined from

$$\mathrm{Re}\left[\int_{Y_m}^{Y} k_Y(\xi)\, d\xi\right] = 0$$

as the *Stokes lines*, and from

$$\mathrm{Im}\left[\int_{Y_m}^{Y} k_Y(\xi)\, d\xi\right] = 0,$$

as the *anti-Stokes lines*. Note that these names are often used vice versa, particularly, in modern fluid dynamics (e.g. Le Dizès et al. [10,31], Yakubenko [11]). The preset order seems to be more correct from the historical point of view. (A discussion of possible sources of the controversy can be found in Olver [36, p. 518].)

If $Y = Y_m$ is a simple zero of $k_Y(Y)$, three Stokes lines and three anti-Stokes lines emerge from it. At the anti-Stokes lines, both solutions (Y_m, Y) and (Y, Y_m) are of the same order of magnitude. In sectors between the anti-Stokes lines, one of the solutions is called dominant—its magnitude is exponentially large (as $Y \to \infty$ inside the sector) compared to the magnitude of the other solution that is called subdominant. When it is important to stress whether the solution (Y_m, Y) is dominant or subdominant, we use the subscripts, i.e. $(Y_m, Y)_d$ or $(Y_m, Y)_s$.

The crucial feature of the WKBJ approximation is the Stokes phenomenon: the general solution cannot be approximated by the same linear combination of (Y_m, Y) and (Y, Y_m) in all three sectors formed by the anti-Stokes lines. The matching procedure that allows one to bypass the problem was suggested originally by Stokes himself. Later on, Heading [35,37] and some others have developed it into a standard tool. The idea of the procedure is as follows.

If the Stokes line is crossed in the positive direction, the approximation changes in the following manner:

$$A(Y_m, Y)_s + B(Y, Y_m)_d \to (A + TB)(Y_m, Y)_s + B(Y, Y_m)_d;$$

at the Stokes line itself, it is

$$\left(A+\frac{1}{2}TB\right)(Y_m,Y)_s+B(Y,Y_m)_d,$$

in which T is called the Stokes multiplier (or Stokes constant). The value of T depends on the order and type of the turning point; for a simple zero of $k_Y(y)$, it is $T=i$. If the approximation is continued across the Stokes line in the opposite direction, T changes to $-T$.

For large positive and negative values of Y from the interval $Y_1<Y<Y_2$, one has $S(Y)\gg 1$. (Actually, the same conclusion is held also for moderate values of Y because $\varepsilon \ll 1$.) Hence, instead of (52), one can use its asymptotic form

$$\zeta=\widetilde{C}S^{-\kappa}e^{S/2}+\widetilde{D}S^{\kappa}e^{-S/2}, \tag{53}$$

in which $\widetilde{C}$ and $\widetilde{D}$ are new arbitrary constants.

The Stokes phenomenon related to (52) and (53) was studied by Heading [37], who obtained the Stokes lines $\arg(S)=\pi l$, the anti-Stokes lines $\arg(S)=\pi(l+1/2)$, in which $l=0,\pm1,\pm2,\ldots,$ and the following Stokes multipliers:

$$T_{2r}=\frac{2\pi i e^{-4\pi i r\kappa}}{\Gamma\left(\frac{1}{2}+\mu+\kappa\right)\Gamma\left(\frac{1}{2}-\mu+\kappa\right)} \tag{54}$$

for even $l=2r$, and

$$T_{2r+1}=\frac{2\pi i e^{2\pi i(2r+1)\kappa}}{\Gamma\left(\frac{1}{2}+\mu-\kappa\right)\Gamma\left(\frac{1}{2}-\mu-\kappa\right)} \tag{55}$$

for odd $l=2r+1$ (Heading [37, p. 201, Eqs (16) and (17)]. Equations (54) and (55) can be combined into the following general formula:

$$T_l=\frac{2\pi i e^{-2\pi i l\nu\kappa}}{\Gamma\left(\frac{1}{2}+\mu+\nu\kappa\right)\Gamma\left(\frac{1}{2}-\mu+\nu\kappa\right)},\quad \nu=(-1)^l. \tag{56}$$

Due to an inadvertence, Heading [37, p. 201, Eq. (18)] put $-4\pi i l\nu\kappa$ in the exponent instead of $-2\pi i l\nu\kappa$. Unfortunately, the resulting incorrect formula has been used by Gavrilenko and Zelekson [8] and BT [9] in their analyses.

6.4. Bypass below

If $k_x>0$, one has $k_x\widetilde{U}'(0)>0$ due to assumption (36). Therefore, the pole $Y=0$ must be bypassed in the lower complex half-plane. This case is mathematically similar to the problem formulated by BT [9]. However, they matched the singularity in the incorrect (upper) half-plane [9, p. 245, figure 6] and used incorrect values of the Stokes multipliers. Therefore, we intend to revise their matching procedure in the following treatment. We choose the branch cuts as shown in *figure 3(a)*, and match the WKBJ approximation around the turning points in the lower complex half-plane, which implies that

$$\arg(k_Y)=\begin{cases}0 & \text{for } Y<Y_1,\\ \pi/2 & \text{for } Y_1<Y<Y_2,\\ \pi & \text{for } Y>Y_2.\end{cases} \tag{57}$$

Equation (49) together with (57) give

$$\kappa = \frac{\varepsilon \widetilde{\Lambda}''(0)}{2k_x \widetilde{\Lambda}'(0)}. \tag{58}$$

The solution of (40) is approximated by

$$\begin{cases} A_1\overrightarrow{(Y_1, Y)} + B_1\overleftarrow{(Y, Y_1)} & \text{for } Y \to -\infty, \\ A_2\overrightarrow{(Y_2, Y)} + B_2\overleftarrow{(Y, Y_2)} & \text{for } Y \to +\infty, \end{cases} \tag{59}$$

in which A_m and B_m are constants.

In a scattering problem, the amplitudes of the waves that propagate away from the region of interaction must be expressed in terms of those of the incoming waves, i.e.

$$[A_2, B_1] = [S]\begin{bmatrix} A_1 \\ B_2 \end{bmatrix}, \tag{60}$$

in which $[S]$ is called the scattering matrix. It can be shown that the matrix has the form

$$[S] = \begin{bmatrix} T & R_2 \\ R_1 & T \end{bmatrix},$$

in which R_1 is the reflection coefficient for the left-scattering problem: $[A_1, B_1] = [1, R_1]$ and $[A_2, B_2] = [T, 0]$, and R_2 is that for the right-scattering one: $[A_1, B_1] = [0, T]$ and $[A_2, B_2] = [R_2, 1]$. Note that the transmission coefficient T is the same even if the flow variation is not symmetric (more details can be found in Mei [21, Section 4.7]).

In our treatment, however, it is more convenient to calculate the reflection and transmission coefficients not from (60) but from the following relation:

$$[A_2, B_2] = [M]\begin{bmatrix} A_1 \\ B_1 \end{bmatrix}, \tag{61}$$

in which

$$[M] = \begin{bmatrix} T - T^{-1}R_1R_2 & T^{-1}R_2 \\ -T^{-1}R_1 & T^{-1} \end{bmatrix}.$$

The details of the matching procedure are given in Appendix B. Thus, the following reflection and transmission coefficients are obtained:

$$R_m = i\nu\Delta^{-1}\left\{1 - \frac{1}{2}\nu\left[\sigma(-\kappa)e^{-2d_1} - \sigma(\kappa)e^{-2d_2}\right] + \frac{1}{4}\left[e^{-2i\pi\kappa} - \sigma(\kappa)\sigma(-\kappa)\right]e^{-2d}\right\}, \tag{62}$$

$$T = \Delta^{-1}e^{-d-i\pi\kappa}, \tag{63}$$

in which $m = 1$ or 2, $\nu = (-1)^m$,

$$\Delta = 1 - \frac{1}{2}\left[\sigma(-\kappa)e^{-2d_1} + \sigma(\kappa)e^{-2d_2}\right] - \frac{1}{4}\left[e^{-2i\pi\kappa} - \sigma(\kappa)\sigma(-\kappa)\right]e^{-2d},$$

$$d_1 = \varepsilon^{-1} \int_{Y_1}^{0} |k_Y(Y)|\, dY, \qquad d_2 = \varepsilon^{-1} \int_{0}^{Y_2} |k_Y(Y)|\, dY, \tag{64}$$

$d = d_1 + d_2$, and

$$\sigma(\kappa) \equiv \frac{\pi}{\Gamma(2-\kappa)\Gamma(-1-\kappa)} \tag{65}$$

with Γ being the Gamma function.

Since $|\kappa| \ll 1$, one has $\sigma(\kappa) = \pi\kappa + \mathrm{O}(\kappa^2)$, and Eqs (62) and (63) can be written as

$$R_m = i\nu\left(1 + \frac{1}{2}e^{-2d} + i\nu\pi\kappa e^{-2d_m}\right) + \mathrm{O}\big(\kappa^2; \kappa e^{-2d}; e^{-4d}\big), \tag{66}$$

$$T = e^{-d}\left[1 - i\pi\kappa - \frac{1}{2}\pi\kappa\big(e^{-2d_1} - e^{-2d_2}\big) + \mathrm{O}\big(\kappa^2; \kappa e^{-d}; e^{-2d}\big)\right]. \tag{67}$$

Equations (66) and (67) yield

$$|R_m|^2 = 1 + e^{-2d} + 2\nu\pi\kappa e^{-2d_m} + \mathrm{O}\big(\kappa^2; \kappa e^{-2d}; e^{-4d}\big), \tag{68}$$

$$|T|^2 = e^{-2d}\big[1 - \pi\kappa e^{-2d_1} + \pi\kappa e^{-2d_2} + \mathrm{O}\big(\kappa^2; \kappa e^{-d}; e^{-2d}\big)\big], \tag{69}$$

and finally

$$|R_m|^2 - |T|^2 = 1 + (-1)^m 2\pi\kappa e^{-2d_m} + \mathrm{O}\big(\kappa^2; \kappa e^{-2d}; e^{-4d}\big),$$

which generalizes the result of KK [6].

6.5. Bypass above

For $k_x < 0$, one has $k_x \widetilde{U}'(0) < 0$. Therefore, the bypass must be taken in the upper complex half-plane. The branch cuts are chosen as shown in *figure 3(b)*, and the branch $k_Y(Y)$ is chosen such that

$$\arg(k_Y) = \begin{cases} 0 & \text{for } Y < Y_1, \\ -\pi/2 & \text{for } Y_1 < Y < Y_2, \\ -\pi & \text{for } Y > Y_2. \end{cases} \tag{70}$$

Equation (49) together with (70) yield

$$\kappa = -\frac{\varepsilon \widetilde{\Lambda}''(0)}{2|k_x|\widetilde{\Lambda}'(0)}, \tag{71}$$

which differs only by the sign from that given by (58). The solution of (40) is approximated by

$$\begin{cases} A_1\overleftarrow{(Y_1, Y)} + B_1\overrightarrow{(Y, Y_1)} & \text{for } Y \to -\infty, \\ A_2\overleftarrow{(Y_2, Y)} + B_2\overrightarrow{(Y, Y_2)} & \text{for } Y \to +\infty. \end{cases}$$

It can be shown that

$$[A_1, B_1] = \big[M(d_2, d_1)\big]\begin{bmatrix} A_2 \\ B_2 \end{bmatrix}, \tag{72}$$

in which $[M]$ are given by (96). Hence, the formulas for the reflection and transmission coefficients can be obtained from (62) and (63) simply by swapping d_1 and d_2. In addition, however, the left- and right-reflection coefficients R_1 and R_2 must be also swapped because (72) expresses $[A_1, B_1]$ in terms of $[A_2, B_2]$, while (61) does vice versa.

6.6. Over-reflection and Landau damping

Since the flow span is infinite and the regions outside the interval (Y_1, Y_2) are wavy, one cannot formally integrate (31) in the y-direction to obtain the total energy of waves per unit length in the x-direction. (Thus, the procedure presented by Takehiro and Hayashi [4, Section 3.3] is not strictly correct.) In a scattering problem, instead of the total energy, one can use the rate of work done in maintaining a wave that continuously transmits the energy into infinity (Craik [32]). This leads to the 'force' approach, since this rate can be related to the energy flux and thus to the Reynolds stress induced by the wave motion. A particularly illuminating example of its use was presented by Lott et al. [19].

In a stability problem, however, the radiation conditions are typically prescribed at both $y \to \pm\infty$. Then, one may argue that the divergence of the total energy can be suppressed by the bottom friction that, although being small, provides the decrease of the waves' amplitudes at large distances. Hence, the arguments of Takehiro and Hayashi [4] can be used. The excitation of the transmitted wave of negative energy increases the energy of the reflected wave compared to that of the incident one, which in its turn results in an increase of the wave amplitude, i.e. in over-reflection. In Eq. (68), it is accounted by the term e^{-2d} that is always positive. Furthermore, this mechanism of over-reflection operates also for non-zero Q' and q, since (68) does not rely on any assumptions about them. Thus, over-reflection can be explained as an interaction between two waves carrying energy of opposite signs (Acheson [33], Ostrovskii et al. [34], Hayashi and Young [23], Stepanyants and Fabrikant [30]).

If the potential vorticity of the basic flow is uniform ($Q' \equiv 0$), Eq. (29) shows that the potential vorticity of the waves is conserved. Two important cases can be distinguished. In the first one, q is zero initially. Then, it is zero at any moment of time (which excludes vorticity waves but retains surface-gravity waves). This case has been discussed in details by Takehiro and Hayashi [4]. In particular, they have shown that over-reflection occurs despite the energy flux being continuous across the critical layer.

For vorticity waves ($q \neq 0$), the other pure kinematic mechanism of the amplification can be at work. It was originally suggested by Orr (for references, see Lindzen [18]). Since the potential vorticity is conserved according to (29), the initial vorticity pattern is simply advected by the basic flow. The advection is different, however, at different spanwise levels because of the basic shear. Let us consider two neighboring points of the local minimum and maximum in the vorticity pattern (figures 5 and 6 of Lindzen [18] are of assistance). If the line that connects the points is tilted initially in the direction opposite to the basic shear, the distance between the points will decrease in time until the line becomes perpendicular to the basic flow velocity. Since the actual values of vorticity at the points are conserved, the distance decrease must lead to the increase of the wave velocity because the vorticity is related to its derivatives. For progressive waves of non-zero potential vorticity, Orr's mechanism can operate effectively only at the regions, where the waves travel with the flow, i.e. in vicinity of critical layers. It worthwhile to note, however, that Takehiro and Hayashi [4] have reported examples of the wave scattering, in which over-reflection occurs in the manner opposite to the Orr mechanism.

Possible direct energy exchange between the waves and fluid particles due to the velocity synchronism near the critical layer is often referred to as Landau damping (it was suggested originally by Landau [27], in plasma physics; see also Briggs et al. [38], Ostrovskii et al. [34], Stepanyants and Fabrikant [30]). Physically, it is related to the trapping of fluid particles (originally electrons) between adjacent peaks. It must be noted, however, that the actual trapping process cannot be accounted completely by the linear theory (for further discussion, see Briggs et al. [38], Craik [32, Section 12], Shrira et al. [39]). The waves interact efficiently with those particles that have velocities from the interval $(c-\delta, c+\delta)$, in which $0<\delta\ll 1$. The difference between the number of particles (per unit length in the x-direction) that propagate faster and slower than the wave can be expressed as

$$N=\bigl[U'(y_c)\bigr]^{-1}\partial_y\left[\frac{H(y)}{U'(y)}\right]_{y=y_c}\delta^2+\mathrm{O}\bigl(\delta^4,\delta^2a^2\bigr), \tag{73}$$

in which a stands for the typical amplitude of disturbances. Equation (73) can be rewritten in terms of the potential vorticity as

$$N\simeq\frac{Q'(y_c)}{U'(y_c)Q^2(y_c)}\delta^2, \tag{74}$$

in which only the leading term is retained. Because of assumption (36), the sign of N coincides with that of the gradient of the basic potential vorticity.

If $N>0$, the waves altogether receive energy due to the interaction. (This extra energy is compensated by the corresponding alterations of the energy of the induced mean flow.) As an example, however, we will discuss the opposite and far more spectacular case, for which the waves carrying negative energy are amplified by transferring energy to the mean flow. Thus, we assume $k_x>0$, the incident wave comes from $+\infty$, and $N<0$. Then, Eqs (58), (4) and (74) together with the condition $Q(y)<0$ give

$$\kappa=\frac{1}{2}k_x^{-1}\delta^{-2}U'(y_c)Q(y_c)N>0. \tag{75}$$

Equations (68) and (69) can be written equivalently as

$$|R_2|^2\simeq 1+2\pi\kappa e^{-2d_2}+e^{-2d}, \tag{76}$$

$$|T|^2\simeq e^{-2d}\bigl[1+\pi\kappa e^{-2d_2}-\pi\kappa e^{-2d_1}\bigr], \tag{77}$$

in which only the leading order terms are retained. The incident and reflected waves carry negative energy, while the transmitted one has positive energy. In reality, the wave transformation near the critical layer involves complex non-linear phenomena (more details and references can be found in Grimshaw [40].) Nevertheless, the structure of formulas (76) and (77) suggests the following, probably oversimplified, scenario. The incident wave ‘enters’ the interaction zone, where it gives energy to the induced mean flow, which leads to increasing of the wave amplitude as accounted by the term $2\pi\kappa e^{-2d_2}$ in (76). Then, it ‘splits’ into the reflected and transmitted waves. (Actually, one may argue that the latter one is emitted rather than transmitted, since its energy is of opposite sign compared to that of the incident wave, Craik [32, Section 5.3].) The amplitude increase that has been already gained affects both waves, thus the term $\pi\kappa e^{-2d_2}$ appears in (77). Furthermore, since the waves carry energy of opposite signs, the amplitude of the reflected one increases additionally, which is accounted by the term e^{-2d} in (76). Finally, as the reflected and transmitted waves in their turn ‘pass through’ the interaction zone, both loose energy. As a result, the amplitude of the reflected one increases (that is why the factor 2 appears in front of $\pi\kappa e^{-2d_2}$ in (76)), while that of the transmitted one decreases, as accounted by the term $-\pi\kappa e^{-2d_1}$ in (77). (Note that the transmission coefficient that was presented by Gavrilenko and Zelekson [8, p. 499, Eq. (10)], does not possess the same anti-symmetry with respect to d_1 and d_2.) In *figure 4*, the reflection

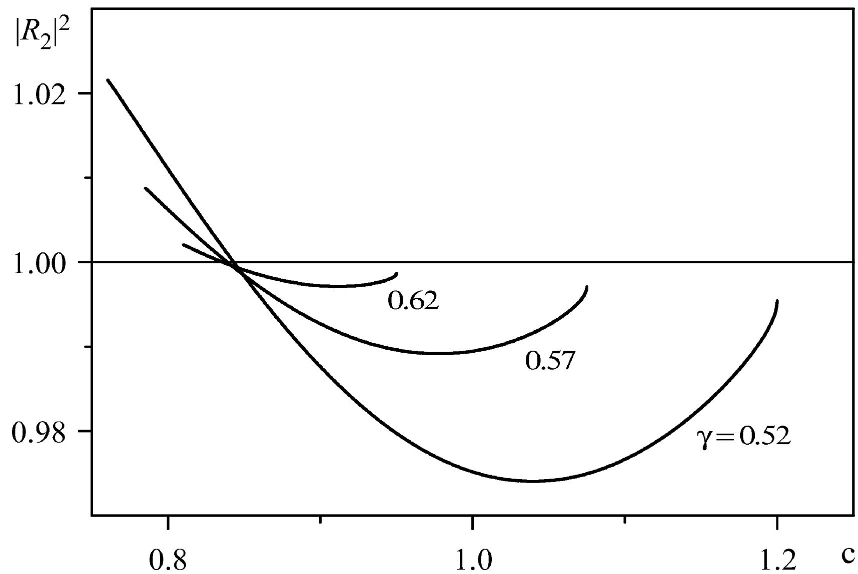

Figure 4. Right-reflection coefficient for tanh-profile of the basic velocity ($U_- = 0.5$, $U_+ = 2.5$, $\varepsilon = 0.03$, and $k_x = 0.06$). Higher values of γ correspond to stronger bottom friction. The interval for the wave phase velocity c is chosen for each value of γ according to (38).

coefficient for the following basic velocity profile is shown

$$U(y) = \frac{1}{2}(U_+ + U_-) + \frac{1}{2}(U_+ - U_-)\tanh(\varepsilon y).$$

Larger values of γ, and thus of the bottom friction, suppress Landau damping.

7. Uniform potential vorticity

The basic flow of uniform potential vorticity presents an important special case, since it sustains over-reflection for any combination of the flow parameters. Actually, for $Q'(y) \equiv 0$, Eq. (74) gives $N \simeq 0$, so that Landau damping is negligible in the leading order approximation. For convenience, we write

$$Q(y) \equiv -U'(y_c)H^{-1}(y_c), \tag{78}$$

in which y_c is the critical layer position. Equation (78) together with (20) give

$$\int_c^{U(y)} \left[\xi f(\xi)\right]^{-1} d\xi = \gamma^2 F^2 U'(y_c)H^{-1}(y_c)(y - y_c),$$

from which $U(y)$ can be found if $f(U)$ is specified. The bottom topography that provides the resulting velocity profile is determined then from (20).

For example, if the Chèzy formula (33) is used, one has

$$H(y) = \left[\frac{c\gamma F}{1 - c^{-1}U'(y_c)(y - y_c)}\right]^2, \qquad U(y) = \frac{c}{1 - c^{-1}U'(y_c)(y - y_c)}. \tag{79}$$

Furthermore, (22) gives $\Lambda(y) = c^{-1}U'(y_c)(y - y_c)$. Therefore, one can make use of the analytic solution obtained by KK [6]. However, in contrast to their case, formulas (79) cannot be applied for the entire y-axis. One can consider instead a piecewise-uniform profile of the potential vorticity, i.e.

$$Q(y) \equiv Q_m \quad \text{for } y \in \mathcal{I}_m\colon\ y_m < y < y_{m+1};$$

for each interval $\mathcal{I}_m$, the bottom and velocity profiles $H_m(y)$ and $U_m(y)$ are given by (79). The general solution of (21) for each interval is similar to that of KK [6], i.e.

$$\hat{h}_m(y) = \left[y - y_c^{(m)}\right]^{1/2}\left\{A_m^{\pm} W_{\kappa,3/4}\left[\xi(y)\right] + B_m^{\pm} W_{-\kappa,3/4}\left[-\xi(y)\right]\right\}, \tag{80}$$

in which

$$\xi(y) \equiv i k_x \nu \left[y - y_c^{(m)}\right]^2,$$

$A_m^{\pm}$ and $B_m^{\pm}$ are constants, $\kappa = -(1/4) i k_x \nu^{-1}$, and $\nu = (c\gamma)^{-1} U_m'[y_c^{(m)}]$. The point $y_c^{(m)}$ is a solution of the equation $U_m(y) = c$. If it is located outside $\mathcal{I}_m$, one can let $A_m^- = A_m^+$ and $B_m^- = B_m^+$. Otherwise, a critical layer occurs at the interval, and different constants must be used at $\mathcal{I}_m^-\colon\ y_m < y < y_c^{(m)}$ and $\mathcal{I}_m^+\colon\ y_c^{(m)} < y < y_{m+1}$. However, they can be related by the analytic continuation formulas for Whittaker's functions (e.g. Olver [36, Section 11.2]). The direction of continuation must be chosen in according to the bypass rule. The constants at the consequent intervals $\mathcal{I}_{m-1}^+$ and $\mathcal{I}_m^-$ can be related if the surface elevation is required to be continuous and smooth at the junctions, which implies $\hat{h}_{m-1}(y_m) = \hat{h}_m(y_m)$ and $\hat{h}'_{m-1}(y_m) = \hat{h}'_m(y_m)$. Finally, it must be kept in mind that vorticity jumps may cause instability even in the absence of critical layers (Stepanyants and Fabrikant [30]).

8. Trapped modes and global instability

The feed-back for the over-reflected wave can be provided by either a lateral boundary of the flow or another critical layer (e.g. Acheson [33], BT [9], Lindzen [18]). The net reflection can lead then to the formation of the so-called trapped modes that are eigenfunctions of Eq. (40), together with the radiation conditions for $y \to \pm\infty$ (Peregrine [41, Section 2.E], Mei [21, Section 4.6]).

For example, two simple but important particular cases are a submerged trough and ridge (*figures 5(a), 5(b)*). In both cases, the scattering potential $P^2(Y)$ may have two critical layers and four turning points (*figure 5(c)*). If the WKBJ approximation can be used in the regions between any two consequent points, the boundary value problem leads to the following relation:

$$\exp\left[i\varepsilon^{-1}\int_{Y_2}^{\widehat{Y}_1} k_Y(k_x,\omega,Y)\,dY\right] R_m\big(\widehat{Y}_1,k_x,\omega\big)\exp\left[-i\varepsilon^{-1}\int_{Y_2}^{\widehat{Y}_1} k_Y(k_x,\omega,Y)\,dY\right] R_m(Y_2,k_x,\omega) = 1, \tag{81}$$

in which

$$k_Y = \left(\frac{[\omega - k_x\widetilde{U}(Y)]^2}{\gamma^2\widetilde{U}^2(Y)} - k_x^2\right)^{1/2}, \tag{82}$$

and the reflection coefficients R_m are given by (62) with $m = 1$ and 2 are taken for the ridge and trough, respectively. Note that the branch of the square root in (82) must be taken such that $\mathrm{Im}(k_Y) > 0$ for $\mathrm{Im}(\omega) > 0$ (see Section 6.1).

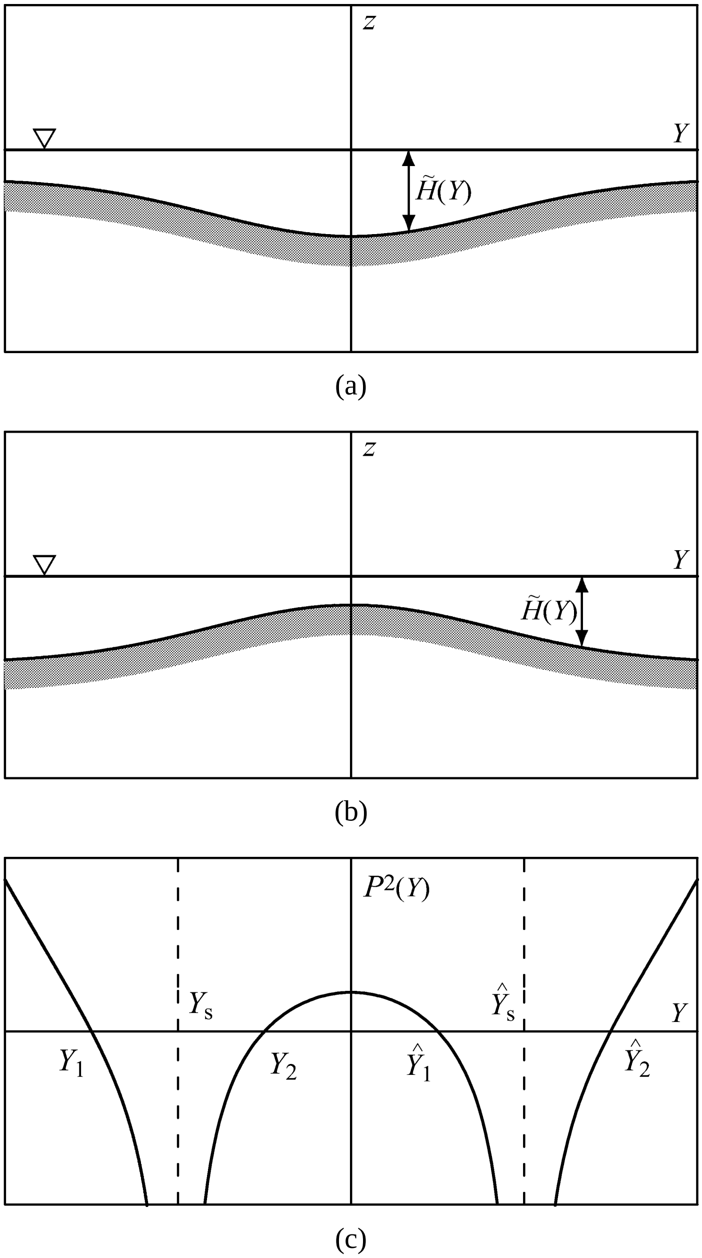

Figure 5. (a) Submerged trough and (b) ridge that may cause the formation of trapped modes; in both cases the corresponding potential, Eq. (40), is similar to that sketched in part (c).

Equation (81) is written in the form that emphasizes the structure of the eigenfunctions. Thus, they are formed by two waves corresponding to $\pm k_Y(k_x, \omega, Y)$, which propagate in the opposite directions at the interval $Y_2 < Y < \widehat{Y}_1$ and are transformed from one into the other at the points Y_2 and $\widehat{Y}_1$. Equation (81) is a requirement that both the amplitude and phase remain unchanged after one or several complete cycles of propagation and reflection. Since such a process must be considered in time, the spatial structure must be in agreement with the temporal variation given by $\exp(-i\omega t)$. Hence, solutions of (81) with respect to ω are the eigenfrequencies.

Taking logarithm of both sides of (81) and separating then real and imaginary parts, one obtains

$$\arg(A) - 2\varepsilon^{-1}\mathrm{Re}\left[\int_{Y_2}^{\widehat{Y}_1} k_Y(k_x, \omega, Y)\,dY\right] = 2\pi n, \tag{83}$$

$$\log|A| - 2\varepsilon^{-1}\mathrm{Im}\left[\int_{Y_2}^{\widehat{Y}_1} k_Y(k_x, \omega, Y)\,dY\right] = 0, \tag{84}$$

in which n is an arbitrary integer, and $A = R_m(\widehat{Y}_1, k_x, \omega) R_m(Y_2, k_x, \omega)$.

For $\mathrm{Im}(\omega) = 0$, Eq. (82) shows that $\mathrm{Im} k_Y(k_x, \omega, Y) = 0$ at the interval $Y_2 < Y < \widehat{Y}_1$. Therefore, the left-hand side of (84) is simply $\log|A| > 0$, and the equation has no solution. Thus, no neutral global modes occur in the case of over-reflection.

For $\mathrm{Im}(\omega) > 0$, one has $\mathrm{Im}(k_Y) > 0$, which means physically that both waves forming the eigenfuction are spatially damped in their direction of propagation. Furthermore, Eq. (82) gives that $\mathrm{Im}(k_Y)$ increases unbounded together with $\mathrm{Im}(\omega)$, while (64) and (68) show that the magnitudes of the reflection coefficients remain finite. Therefore, one can easily chose $\mathrm{Im}(\omega) > 0$ to satisfy (84) for any value of $\mathrm{Re}(\omega)$ that provides the required location of the turning points. This gives certain curves on the complex ω plane. Actual eigenfrequencies are located at distances of order ε near these curves (Kulikovskii [43]). To develope an appreciation of this fact, one might note that (83) and (84) present the balance of phase and amplitude, respectively. The first is often called the quantization condition (Heading [35]). Roughly speaking, it states that the distance between Y_2 and $\widehat{Y}_1$ must be multiple of a certain number of wave-lengths. Since this distance must be much larger than the typical wave-length (as required by the WKBJ approximation), the phase balance can be easily achieved by small variation of ω after the amplitude balance is established.

Since the magnitudes of the reflection coefficients are only slightly larger that unity, one can expect eigenfrequencies with $0 < \mathrm{Im}(\omega) \ll 1$. Series expansions of (82), (83) and (84) for small $\mathrm{Im}(\omega)$ lead then to the so-called laser formula, from which the eigenfrequencies can be calculated approximately (Acheson [33, Appendix B], Takehiro and Hayashi [4], KK [6]). Thus, one has instead of (84) the following expression:

$$\mathrm{Im}(\omega) \simeq \frac{1}{2}\varepsilon\gamma \log|A| \left\{ \int_{Y_2}^{\widehat{Y}_1} \left(\frac{1}{\widetilde{U}^2(Y)} - \frac{\gamma^2 k_x^2}{[\mathrm{Re}(\omega) - k_x \widetilde{U}(Y)]^2} \right)^{-1/2} dY \right\}^{-1}, \tag{85}$$

in which A, Y_2 and $\widehat{Y}_1$ must be calculated for the same value of $\mathrm{Re}(\omega)$ but $\mathrm{Im}(\omega) = 0$. Equation (85) clearly indicates $\mathrm{Im}(\omega) > 0$ if $|A| > 0$, i.e. in the case of over-reflection.

In the theory of stability of parallel flows, Eq. (81) is the dispersion relation between the wavenumber k_x and frequency ω. Thus, if one has $\mathrm{Im}\omega(k_x) > 0$ for at least one real value of k_x, the corresponding eigenfunction is a self-exited normal mode.

Alternatively, k_x can be treated merely as a parameter in (81), and the stability problem is considered for a fictitious flow that is one-dimensional and spatially developing. Then, $k_Y(k_x, \omega, Y)$ presents the local wave number, and (82) is the local dispersion. In this approach, the solutions of (81) with respect to ω and the corresponding eigenfunctions $\tilde{h}(Y)$ are called global frequencies and global modes, respectively (more details can be found in Huerre and Monkewitz [13], Le Dizès et al. [10], Yakubenko [11]). The dispersion relation (82) indicates no local instability. (Moreover, we have assumed the region of the flow parameters for which the local hydraulic instability would never occur even if we retained the terms due to the bottom friction.) Nevertheless, some of the eigenfrequencies have positive imaginary parts, and the flow is globally unstable.

9. Conclusions and discussion

Two types of instability can occur in a shallow stream down a non-uniform slope. Although both have a similar origin, that is the flow shear, either normal or lateral, their appearances and features are different in the framework of the shallow-water approximation. If the basic flow varies weakly in the spanwise direction, the classic hydraulic instability due to the bottom friction can be treated at every spanwise position by means of the local analysis. A region of parameters exists, for which the flow is locally stable everywhere. However, in the case of instability, the waves of infinitely short wavelength are the most amplified, which contradicts the long-wave nature of the shallow-water approximation. As we showed elsewhere (Yakubenko and Shugai [16]), the problem can be resolved completely if the internal lateral friction is taken into account. The price is that some other higher order terms must be retained, and thus the Saint Venant shallow-water equations must be abandoned.

It the present paper we have analyzed the wave scattering problem and linear shear instability for the case of small slope and bottom friction, and weak spanwise variation of the basic flow. The wave propagation can be studied then by means of the frictionless linearized Saint Venant equations, at least in the range of the flow parameters for which the hydraulic instability cannot occur. However, the velocity profile of the basic flow and the bottom topography remain related uniquely by the bottom friction.

The energy of the total perturbed flow can be split into three main parts that are related to the basic flow, small amplitude wave motion, and induced mean flow. The instability is related then to the amplification or damping of the waves near the critical layers, where their streamwise phase speed coincides with the velocity of the basic flow. Two physical mechanisms of this amplification exist. The first one is similar to that suggested by Takehiro and Hayashi [4] in frictionless shallow water; it is due to the fact that the incident and transmitted waves carry energy of opposite sign, which results in an increase of the amplitude of the reflected wave compared to that of the incident one. This process occurs for any combination of the flow parameters, and it is often referred to as the wave over-reflection. The other mechanism is Landau damping due to the energy exchange between the waves and fluid particles. It may lead to either additional amplification or damping of the waves for different parameters of the flow. In particular, its significance can be reduced by stronger bottom friction. For a basic flow of uniform potential vorticity, Landau damping is negligible in the leading order approximation. Furthermore, over-reflection occurs then without any exchange of energy between the waves and induced mean flow.

If the proper feed-back is provided by another critical layer, the net over-reflection results into the formation of self-excited trapped modes, which can be interpreted as the global instability of a one-dimensional state that is spatially developing and has no region of local instability.

In the case studied in the present paper, the growth rates are small, and the instability of marginal nature. However, a similar conclusion can be based on the classic Kelvin–Helmholtz instability that also involves interaction between waves that carry energy of opposite signs, even thought the critical layer is replaced by an infinitely thin vortex sheet (Acheson [33], Lindzen [18]). The reflection coefficient can be significantly larger than unity (Stepanyants and Fabrikant [30]). As a result, some of the eigenfrequencies corresponding to the trapped modes have finite $\mathrm{Im}(\omega) > 0$, and the related global instability is not necessary marginal.

As a conclusion, a region of local instability is not necessary for the flow to be globally unstable if the wave amplification is caused by a localized singularity (e.g. a critical layer) that does not alter the total wave energy, but can separate the waves carrying energy of different signs. To our knowledge, however, the question whether over-reflection is possible in a real one-dimensional flow remains open.

Finally, we would like to point out that the fundamental work by Heading [37] has to be corrected. The general formula for the Stokes multiplier (Heading [37, p. 201, Eq. (18)]) should look like our Eq. (56).

Unfortunately, the incorrect formula has been used already in the analyses of Gavrilenko and Zelekson [8], Basovich and Tsimring [9].

Appendix A. More analytically solvable cases?

Equation (14) can be rewritten as

$$\partial_y(\Lambda^2) - k_x^2 F^2 \hat{h}(\hat{h}')^{-1}\Lambda^4 + (k_x^2\hat{h} - \hat{h}'')(\hat{h}')^{-1}\Lambda^2 = 0, \tag{86}$$

which is Bernoulli's equation for Λ^2 (see e.g. Polyanin and Zaitsev [42]).

Its solution can be presented as

$$\Lambda^2(y) = \frac{\hat{h}'(y)G(y)}{C - k_x^2 F^2 \int \hat{h}(y)G(y)\,dy}, \tag{87}$$

in which

$$G(y) = \exp\left\{-k_x^2 \int \hat{h}(y)\left[\hat{h}'(y)\right]^{-1} dy\right\},$$

and C is an arbitrary constant. Using (87), one can investigate systematically for which profiles of the bottom and undisturbed velocity, a disturbance of the given shape $\hat{h}(y)$ can occur.

For example, if $\hat{h}(y) = \tilde{h}\exp(ik_y y)$, Eq. (87) yields

$$\Lambda^2(y) = \left\{\frac{k_x^2 F^2}{k_x^2 + k_y^2} - i\frac{C}{k_y\tilde{h}}\exp\left[-i\left(k_x^2 + k_y^2\right)k_y^{-1} y\right]\right\}^{-1},$$

which gives a one-parameter set of periodic solutions; the uniform solution corresponds to $C = 0$.

Appendix B. Matching procedure

This appendix gives a revision of the matching procedure presented by BT [9]. The numbers correspond to the domains of the complex Y plane shown in *figure 3(a)*. Matching around the turning point Y_2 gives

$$\begin{aligned}
&1: \quad A_2(Y_2, Y)_s + B_2(Y, Y_2)_d,\\
&2: \quad (A_2 - iB_2)(Y_2, Y)_s + B_2(Y, Y_2)_d,\\
&3: \quad (A_2 - iB_2)(Y_2, Y)_d + B_2(Y, Y_2)_s,\\
&3\text{–}4: \quad (A_2 - iB_2)(Y_2, Y)_d + \left[B_2 - \frac{1}{2}i(A_2 - iB_2)\right](Y, Y_2)_d = C_2(0, Y)_d + D_2(Y, 0)_s,
\end{aligned} \tag{88}$$

in which

$$[A_2, B_2] = \begin{bmatrix} 1/2 & i \\ (1/2)i & 1 \end{bmatrix} \begin{bmatrix} e^{-d_2} & 0 \\ 0 & e^{d_2} \end{bmatrix} \begin{bmatrix} C_2 \\ D_2 \end{bmatrix} \tag{89}$$

with d_2 given by (64).

Similar matching around the turning point Y_1 gives:

$$
\begin{aligned}
12&: \quad A_1(Y_1, Y)_d + B_1(Y, Y_1)_s,\\
11&: \quad A_1(Y_1, Y)_d + (B_1 + iA_1)(Y, Y_1)_s,\\
10&: \quad A_1(Y_1, Y)_s + (B_1 + iA_1)(Y, Y_1)_d,\\
9-10&: \quad \left[A_1 + \frac{1}{2}i(B_1 + iA_1)\right](Y_1, Y)_s + (B_1 + iA_1)(Y, Y_1)_d = C_1(0, Y)_s + D_1(Y, 0)_d,
\end{aligned}
\tag{90}
$$

in which

$$
[C_1, D_1] = \begin{bmatrix} e^{-d_1} & 0 \\ 0 & e^{d_1} \end{bmatrix} \begin{bmatrix} 1/2 & (1/2)i \\ i & 1 \end{bmatrix} \begin{bmatrix} A_1 \\ B_1 \end{bmatrix}
\tag{91}
$$

with d_1 given by (64).

At line 6–7, the solution is approximated by (50) that together with (53) can be written as

$$
6-7: \quad C_0 S^{-\kappa}(0, Y) + D_0 S^{\kappa}(Y, 0).
$$

Matching around the origin gives then

$$
\begin{aligned}
6&: \quad C_0 S^{-\kappa}(0, Y)_s + D_0 S^{\kappa}(Y, 0)_d,\\
5-6&: \quad \left(C_0 + \frac{1}{2}T_1 D_0\right) S^{-\kappa}(0, Y)_s + D_0 S^{\kappa}(Y, 0)_d,
\end{aligned}
\tag{92}
$$

in which T_1 is given by (56) with $l = 1$. For large (and moderate) values of Y from the interval $[0, Y_2]$, one has $|S| \gg 1$ and $\arg(S) = \pi$. Therefore, $S^{-\kappa}(0, Y) \simeq e^{-i\pi\kappa}(0, Y)$ and $S^{\kappa}(Y, 0) \simeq e^{i\pi\kappa}(Y, 0)$. Equations (88) and (89) give then

$$
[C_2, D_2] = \begin{bmatrix} e^{-i\pi\kappa} & (1/2)T_1 e^{-i\pi\kappa} \\ 0 & e^{i\pi\kappa} \end{bmatrix} \begin{bmatrix} C_0 \\ D_0 \end{bmatrix}.
\tag{93}
$$

Similar matching in the other direction gives

$$
\begin{aligned}
7&: \quad C_0 S^{-\kappa}(0, Y)_d + D_0 S^{\kappa}(Y, 0)_s,\\
7-8&: \quad C_0 S^{-\kappa}(0, Y)_d + \left(D_0 - \frac{1}{2}T_0 C_0\right) S^{\kappa}(Y, 0)_s,
\end{aligned}
\tag{94}
$$

in which T_0 is given by (56) with $l = 0$. For large (and moderate) negative values of Y from the interval $Y_1 < Y < 0$, one has $|S| \gg 1$ and $\arg(S) = 0$. Therefore, $S^{-\kappa}(0, Y) \simeq (0, Y)$, $S^{\kappa}(Y, 0) \simeq (Y, 0)$, and Eqs (90) and (91) give

$$
[C_0, D_0] = \begin{bmatrix} 1 & 0 \\ (1/2)T_0 & 1 \end{bmatrix} \begin{bmatrix} C_1 \\ D_1 \end{bmatrix}.
\tag{95}
$$

Equations (89), (91), (93) and (95) yield straightforwardly

$$
\left[M(d_1, d_2)\right] = \begin{bmatrix} (1/2)e^{-d_2} & ie^{d_2} \\ (1/2)ie^{-d_2} & e^{d_2} \end{bmatrix} \begin{bmatrix} e^{-i\pi\kappa} - \sigma(\kappa)\sigma(-\kappa)e^{i\pi\kappa} & i\sigma(\kappa)e^{i\pi\kappa} \\ i\sigma(-\kappa)e^{i\pi\kappa} & e^{i\pi\kappa} \end{bmatrix} \begin{bmatrix} (1/2)e^{-d_1} & (1/2)ie^{-d_1} \\ ie^{d_1} & e^{d_1} \end{bmatrix},
\tag{96}
$$

in which $\sigma(\kappa)$ is given by (65).

Acknowledgements

Several discussions with A.G. Kulikovskii, I.S. Shikina, A.D. Polyanin and K.G. Kornev are acknowledged. This work has been supported by The Royal Swedish Academy of Sciences (Project no. 1264).

References

[1] Jeffreys H., The flow of water in an inclined channel of rectangular cross-section, Philos. Mag. Ser. 6 49 (1925) 793.
[2] Satomura T., An investigation of shear instability in shallow water, J. Met. Soc. Jpn 59 (1981) 148–167.
[3] Chu V.H., Wu J.-H., Khayat R.E., Stability of transverse shear flow in shallow open channels, J. Hydraul. Eng-ASCE 117 (1991) 1370–1388.
[4] Takehiro S.I., Hayashi Y.-Y., Over-reflection and shear instability in shallow water model, J. Fluid Mech. 236 (1992) 259–279.
[5] Dodd N., On the destabilization of a longshore current on a plane beach: Bottom shear stress, critical condition, and onset of instability, J. Geophys. Res. 99 (1994) 811–824.
[6] Knessl C., Keller J.B., Stability of linear shear flow in shallow water, J. Fluid Mech. 303 (1995) 203–214.
[7] Knessl C., Keller J.B., Stability of rotating shear flows in shallow water, J. Fluid Mech. 244 (1992) 605–614.
[8] Gavrilenko V.G., Zelekson L.A., Sound amplification in nonuniform flow, Sov. Phys. Acoust. 23 (1977) 497–500.
[9] Basovich A.Y., Tsimring L.Sh., Internal waves in a horizontally inhomogeneous flow, J. Fluid Mech. 142 (1984) 233–249.
[10] Le Dizès S., Huerre P., Chomaz J.-M., Monkewitz P.A., Linear global modes in spatially developing media, Philos. T. Roy. Soc. A 354 (1996) 169–212.
[11] Yakubenko P.A., Global capillary instability of an inclined jet, J. Fluid Mech. 346 (1997) 181–200.
[12] Brevdo L., Bridges T.J., Local and global instabilities of spatially developing flows: cautionary examples, P. Roy. Soc. Lond. A Mat. 453 (1997) 1345–1364.
[13] Huerre P., Monkewitz P.A., Local and global instabilities in spatially developing flows, Annu. Rev. Fluid Mech. 22 (1990) 473–537.
[14] Grubišić V., Smith R.B., The effect of bottom friction on shallow-water flow past an isolated obstacle, J. Atmos. Sci. 52 (1995) 1985–2005.
[15] Chen D., Jirka G.H., Absolute and convective instabilities of a plane turbulent wakes in a shallow water layer, J. Fluid Mech. 338 (1997) 157–172.
[16] Yakubenko P.A., Shugai G.A., Note on two-dimensional instability in shallow-water flows, Acta Mech. 135 (1999) 101–112.
[17] Booker J.R., Bretherton F.P., The critical layer for internal gravity waves in a shear flow, J. Fluid Mech. 27 (1967) 513–539.
[18] Lindzen R.S., Instability of plane parallel shear flow, Pure Appl. Geophys. 126 (1988) 103–121.
[19] Lott F., Kelder H., Teitelbaum H., A transition from Kelvin–Helmholtz instability to propagating wave instability, Phys. Fluids A-Fluid 4 (1992) 1990–1997.
[20] Zhuang M., Dimotakis P.E., Kubota T., The effect of walls on a spatially growing supersonic shear layer, Phys. Fluids A-Fluid 2 (1990) 599–604.
[21] Mei C.C., The Applied Dynamics of Ocean Surface Waves, World Scientific, Singapore, 1989.
[22] Drazin P.G., Davey A., Shear layer instability of an inviscid compressible fluid. Part 3, J. Fluid Mech. 82 (1977) 252–260.
[23] Hayashi Y.-Y., Young W.R., Stable and unstable shear modes of rotating parallel flows in shallow water, J. Fluid Mech. 184 (1987) 477–504.
[24] McPhaden M.J., Ripa P., Wave-mean flow interaction in the equatorial ocean, Annu. Rev. Fluid Mech. 22 (1990) 167–205.
[25] Henningson D.S., Gustavsson L.H., Breuer K.S., Localized disturbances in parallel shear flows, Appl. Sci. Res. 53 (1994) 51–97.
[26] Grimshaw R., A general theory of critical level absorption and valve effects for linear wave propagation, Geophys. Astro. Fluid 14 (1980) 303–326.
[27] Landau L.D., On the vibrations of the electronic plasma, J. Phys. 10 (1946) 25–34.
[28] Lin C.C., The Theory of Hydrodynamic Stability, Cambridge University Press, Cambridge, 1955.
[29] Boyd J.P., Complex coordinate methods for hydrodynamic instabilities and Sturm–Liouville eigenproblems with an interior singularity, J. Comput. Phys. 57 (1985) 454–471.
[30] Stepanyants Yu.A., Fabrikant A.L., Propagation of waves in hydrodynamic shear flows, Sov. Phys. Usp. 32 (1989) 783–805.
[31] Le Dizès S., Monkewitz P.A., Huerre P., Viscous structure of plane waves in spatially developing shear flows, Phys. Fluids 7 (1995) 1337–1347.
[32] Craik A.D.D., Wave Interaction and Fluid Flow, Cambridge University Press, Cambridge, 1985.
[33] Acheson D.J., On over-reflection, J. Fluid Mech. 77 (1976) 433–472.
[34] Ostrovskii S.A., Rybak S.A., Tsimring L.Sh., Negative energy waves in hydrodynamics, Sov. Phys. Usp. 29 (1986) 1040–1052.
[35] Heading J., An Introduction to Phase-Integral Methods, Methuen, London, 1962.
[36] Olver F.W.J., Asymptotics and Special Functions, Academic Press, New York, 1974.
[37] Heading J., The Stokes phenomenon and the Whittaker function, J. Lond. Math. Soc. 37 (1962) 195–208.
[38] Briggs R.J., Daugherty J.D., Levy R.H., Role of Landau damping in crossed-field electron beams and inviscid shear flow, Phys. Fluids 12 (1970) 421–432.
[39] Shrira V.I., Voronovich V.V., Kozhelupova N.G., Explosive instability of vorticity waves, J. Phys. Oceanogr. 27 (1997) 542–554.
[40] Grimshaw R., Resonant wave interaction near a critical layer in a stratified shear flow, J. Fluid Mech. 269 (1994) 1–22.
[41] Peregrine D.H., Interaction of water waves and currents, Adv. Appl. Mech. 16 (1972) 9–117.

[42] Kulikovskii A.G., On the stability conditions for stationary states or flows in regions extended in one direction, J. Appl. Math. Mech. 49 (1985) 316–321.
[43] Polyanin A.D., Zaitsev V.Z., Handbook of Exact Solutions for Ordinary Differential Equations, CRC Press, 1995.